



## Article

# The Grain for Green Program Intensifies Trade-Offs between Ecosystem Services in Midwestern Shanxi, China

Baoan Hu <sup>1</sup>, Zhijie Zhang <sup>2</sup>, Hairong Han <sup>1,\*</sup> , Zuzheng Li <sup>3</sup>, Xiaoqin Cheng <sup>1</sup>, Fengfeng Kang <sup>1</sup> and Huifeng Wu <sup>1</sup>

<sup>1</sup> School of Ecology and Nature Conservation, Beijing Forestry University, Beijing 100083, China; baoanhu@bjfu.edu.cn (B.H.); cloud2014@bjfu.edu.cn (X.C.); phoonkong@bjfu.edu.cn (F.K.); huifengwu@bjfu.edu.cn (H.W.)

<sup>2</sup> Hohhot Meteorological Bureau, Hohhot 010020, China; zhzhj1982@163.com

<sup>3</sup> State Key Laboratory of Urban and Regional Ecology, Research Center for Eco-Environmental Sciences, Chinese Academy of Sciences, Beijing 100085, China; zuzhengli@rcees.ac.cn

\* Correspondence: hanhr6015@bjfu.edu.cn; Tel.: +86-010-62336015

**Abstract:** Ecological engineering is a widely used strategy to address environmental degradation and enhance human well-being. A quantitative assessment of the impacts of ecological engineering on ecosystem services (ESs) is a prerequisite for designing inclusive and sustainable engineering programs. In order to strengthen national ecological security, the Chinese government has implemented the world's largest ecological project since 1999, the Grain for Green Program (GFGP). We used a professional model to evaluate the key ESs in Lvliang City. Scenario analysis was used to quantify the contribution of the GFGP to changes in ESs and the impacts of trade-offs/synergy. We used spatial regression to identify the main drivers of ES trade-offs. We found that: (1) From 2000 to 2018, the contribution rates of the GFGP to changes in carbon storage (CS), habitat quality (HQ), water yield (WY), and soil conservation (SC) were 140.92%, 155.59%, −454.48%, and 92.96%, respectively. GFGP compensated for the negative impacts of external environmental pressure on CS and HQ, and significantly improved CS, HQ, and SC, but at the expense of WY. (2) The GFGP promotes the synergistic development of CS, HQ, and SC, and also intensifies the trade-off relationships between WY and CS, WY and HQ, and WY and SC. (3) Land use change and urbanization are significantly positively correlated with the WY–CS, WY–HQ, and WY–SC trade-offs, while increases in NDVI helped alleviate these trade-offs. (4) Geographically weighted regression explained 90.8%, 94.2%, and 88.2% of the WY–CS, WY–HQ, and WY–SC trade-offs, respectively. We suggest that the ESs' benefits from the GFGP can be maximized by controlling the intensity of land use change, optimizing the development of urbanization, and improving the effectiveness of afforestation. This general method of quantifying the impact of ecological engineering on ESs can act as a reference for future ecological restoration plans and decision-making in China and across the world.

**Keywords:** Grain for Green Program; ecosystem services trade-offs; scenario analysis; spatial regression; Midwestern Shanxi



**Citation:** Hu, B.; Zhang, Z.; Han, H.; Li, Z.; Cheng, X.; Kang, F.; Wu, H. The Grain for Green Program Intensifies Trade-Offs between Ecosystem Services in Midwestern Shanxi, China. *Remote Sens.* **2021**, *13*, 3966. <https://doi.org/10.3390/rs13193966>

Academic Editors: Baojie He, Ayyoob Sharifi, Chi Feng and Jun Yang

Received: 30 August 2021

Accepted: 30 September 2021

Published: 3 October 2021

**Publisher's Note:** MDPI stays neutral with regard to jurisdictional claims in published maps and institutional affiliations.



**Copyright:** © 2021 by the authors. Licensee MDPI, Basel, Switzerland. This article is an open access article distributed under the terms and conditions of the Creative Commons Attribution (CC BY) license (<https://creativecommons.org/licenses/by/4.0/>).

## 1. Introduction

Ecosystem services (ESs) refer to all the benefits that human beings obtain directly or indirectly from the natural ecosystem to meet and maintain their living needs [1,2]. The Millennium Ecosystem Assessment (MEA) divides ESs into four basic types, including regulating services (e.g., soil conservation and carbon storage), provisioning services (e.g., water and timber), supporting services (e.g., biodiversity conservation and nutrient cycling), and cultural services (e.g., forest recreation) [2,3]. Human development patterns over the last few centuries have detrimentally affected the health and resilience of natural ecosystems [3,4]. Declines in ESs have been observed at global and regional scales, and these declines pose a significant threat to human well-being [2,5]. Ecological engineering is a widely adopted countermeasure that attempts to mitigate the contradiction between human

development and ecosystem protection [6,7]. Ecological engineering aims to increase the sustainable supply of ESs by repairing or improving ecosystem functioning [8,9]. At present, global investment in the development of ecological engineering amounts to billions of dollars per year [9], and quantitative assessment of the effects of ecological engineering on ESs has attracted the attention of many managers, research organizations, and researchers [10].

ESs are good indicators for evaluating the ecological benefits of ecological engineering, as they effectively connect human well-being and the natural environment [1,11]. ES trade-offs occur when the increase of a certain ES is at the cost of reducing another ES [2,12]. Therefore, revealing the influencing factors of ES trade-offs is crucial to maintaining the sustainable supply of multiple ESs [12,13]. The frequent conversion between land use types caused by high-intensity human activities is the main cause of ES declines [14,15]. Rebuilding the ecological functioning of degraded ecosystems by changing land use patterns and intensity of use is the main aim of most ecological projects [8,16], which will have strong impacts on the supply and trade-offs between ESs [17,18]. Ecological engineering that unilaterally promotes a single ES makes it difficult to maximize ecological benefits [19], and may even negatively affect ecosystem functioning and cause other services to decline [20,21].

Ecological degradation is one of the main reasons for the increasing frequency of natural disasters [22]. In order to achieve carbon neutrality and strengthen national ecological security, the Chinese government has implemented the world's largest ecological project since 1999: the Grain for Green Program (GFGP) [23]. With the implementation of the GFGP, vegetation cover has increased significantly [24] and various ESs, such as biodiversity and climate regulation, have been significantly improved [25]. However, large-scale planting of non-native vegetation not only leads to a significant increase in water consumption and evapotranspiration [26], which aggravates the potential conflict between regional ecosystem functioning and human demand for water resources [27], but also further challenges the achievement of balance between green and grain land, especially in arid regions [28,29]. This has rendered uncertain the sustainability of the ecological benefits of the GFGP. Therefore, quantitative assessment of the impacts of ecological engineering on ESs and analysis of the dominant factors driving ES trade-offs are prerequisites for the design of inclusive and sustainable ecological engineering [30].

In the context of rapid socio-economic development, most studies have confirmed that the GFGP can improve ESs and change the relationship between ecosystem support services and regulation services [31,32]. However, this change is influenced by multiple factors, such as natural, anthropogenic, climatic, and socio-economic factors [33]. There are few studies that quantify the contribution rate of ecological engineering to changes in ESs and the impacts of ecological engineering on the relationship between different ESs. In this study, we focus on Lvliang City, Shanxi Province, an area typical of the GFGP. This region has serious soil erosion and is a typical ecologically fragile zone. Our specific objectives are: (1) to quantify the contribution rate of the GFGP to changes in ESs; (2) to analyze the impacts of the GFGP on the trade-offs and synergy between ESs; and (3) to identify the factors influencing the trade-offs between ESs and put forward suggestions for promoting the inclusive and sustainable development of the GFGP. This research should serve as a reference for future ecological engineering projects in China and around the world.

## 2. Materials and Methods

### 2.1. Study Area

Lvliang City is located in the east-central region of China's Loess Plateau and the western region of Shanxi Province, and has an area of about 21,100 km<sup>2</sup> (Figure 1). Lvliang City has a continental monsoon climate with four distinct seasons, synchronized rain and heat, and sufficient sunlight. The average annual temperature is between 0.4 °C and 12.2 °C, and the average annual precipitation is between 438 and 588 mm. The elevation of the study area ranges from 561 to 2806 m a.s.l., with high terrain in the middle of the study area and lower terrain on the edges (Figure 1). Vegetation cover in the mountains of the central

and eastern regions is relatively high, and human activities and industrial development are mainly concentrated in the southeastern plains; the western loess hilly regions have broken terrain, barren soil, and sparse vegetation [34,35]. Due to the low coverage rate of surface vegetation coupled with the landform type of prevalent ravines, the area has serious soil erosion and is typically an ecologically fragile area [34]. In recent years, because of the GFGP, the vegetation coverage rate in this area has increased significantly, the functions of various ecosystems such as climate regulation and soil conservation have improved significantly, and ESs have, accordingly, changed significantly [24,35].

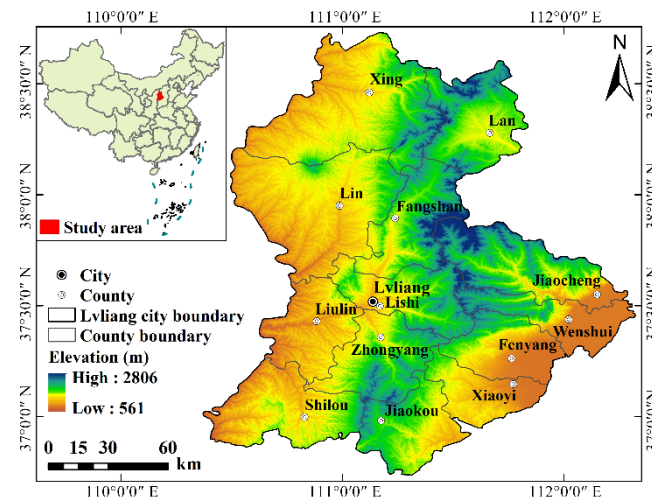


**Figure 1.** Location and elevation of study area.

## 2.2. Data Sources and Descriptions

In this study, we used multi-source data products, such as land use, meteorology, soil, and digital elevation models, to evaluate ESs. Detailed descriptions and data sources are shown in Table 1. In ArcGIS 10.2, all data are converted to the same projected coordinate system (WGS\_1984\_UTM\_Zone\_49N), and the “Resample” tool is used to unify the raster data resolution to 30 m.

**Table 1.** Description and sources of data used to evaluate ESs.

Data	Data Format	Data Description	Data Sources
Land use maps	Raster (30 m)	Land use maps interpreted from Landsat TM/ETM/OLI images. Land use types are classified into seven categories: farmland, forest, grassland, shrub land, water body, construction land, and unused land.	Data Center for Resources and Environmental Sciences, Chinese Academy of Sciences ( <a href="http://www.resdc.cn/">http://www.resdc.cn/</a> (accessed on 16 March 2021))
Digital Elevation Model	Raster (30 m)	Elevation data.	Geospatial Data Cloud ( <a href="http://www.gscloud.cn">http://www.gscloud.cn</a> (accessed on 16 March 2021))
Meteorological data	Raster (1 km)	Including monthly average temperature and precipitation, annual average temperature and precipitation, and potential evapotranspiration.	National Earth System Science Data Center ( <a href="http://www.geodata.cn/">http://www.geodata.cn/</a> (accessed on 16 March 2021))
Soil properties	Raster (1 km)	Including soil texture, topsoil sand fraction, topsoil silt fraction, topsoil clay fraction, topsoil organic carbon, root restricting layer depth, and plant available water content.	Harmonized World Soil database ( <a href="http://www.iiasa.ac.at/Research/LUC/External-World-soil-database/HTML/">http://www.iiasa.ac.at/Research/LUC/External-World-soil-database/HTML/</a> (accessed on 16 March 2021))

Table 1. Cont.

Data	Data Format	Data Description	Data Sources
Evapotranspiration coefficient (Kc)	Excel format	Plant evapotranspiration for different land use types.	Food and Agriculture Organization of the United Nations (FAO) ( <a href="http://www.fao.org/3/X0490E/x0490e0b.htm">http://www.fao.org/3/X0490E/x0490e0b.htm</a> ) (accessed on 16 March 2021)
Watershed boundary	Shapefile	Digital watershed atlas.	HydroSHEDS ( <a href="http://hydrosheds.org/">http://hydrosheds.org/</a> ) (accessed on 16 March 2021)

### 2.3. Quantifying Ecosystem Services

The InVEST model is used to quantify four key ESs: water yield (WY), soil conservation (SC), habitat quality (HQ), and carbon storage (CS). WY is calculated based on the difference between annual average precipitation and actual annual evapotranspiration [29,36]. SC refers to the erosion control ability of the ecosystem to prevent soil loss and the ability to store and maintain sediment [36,37]. The sediment delivery ratio module calculates soil conservation services based on the difference between potential (under extremely degraded conditions without vegetation cover) and actual (under current land cover and management conditions) soil loss [19,36,37]. HQ refers to the ability to provide resources and environmental conditions for the survival and development of species or populations, which depends on the abundance of natural resources [36,38]. The habitat quality module calculates the HQ according to the habitat suitability of each land use type, the impact distance and weight of threat factors, and the sensitivity of each land use type to threat factors [36,38]. Through previous studies [38–41], we determined the impact distance and weight of threat factors, the habitat suitability of each land use type, and the sensitivity parameters to each threat factor (Tables S1 and S2). The carbon module quantifies CS using previous local research on the carbon density of different land use types [42–44] (Table S3). To avoid the influence of abnormal climate fluctuations in a single year, we selected the average rainfall and temperature from 2000 to 2018 as the general results from the study area [45,46]. Table 2 provide greater detail on the process of assessment of each ES.

Table 2. Methods for quantifying ESs.

ESs	Methods	Mathematical Expression
WY	InVEST model water yield module	$WY_x = (1 - AET_x/P_x) \times P_x$ <p><math>WY_x</math>: annual water yield for each grid cell; <math>AET_x</math>: annual actual evapotranspiration for pixel <math>x</math>; <math>P_x</math>: annual precipitation on pixel <math>x</math>; Biophysical coefficients of model input are shown in Table S3.</p>
SC	InVEST model sediment delivery ratio module	$SC = R \times K \times LS \times (1 - C \times P)$ <p><math>SC</math>: soil conservation; <math>R</math>: rainfall erosion factor; <math>K</math>: soil erosion factor; <math>LS</math>: slope length and gradient factor; <math>C</math>: vegetation cover factor; <math>P</math>: support practice factor. <math>R</math> and <math>K</math> are calculated to refer to the method of Yang et al. [32] and Zhang et al. [37]. We assigned <math>C</math> and <math>P</math> values according to existing literature [17,36,39] (Table S3).</p>
HQ	InVEST model habitat quality module	$HQ = H_j \times \left[ 1 - \left( \frac{D_{xj}^Z}{D_{xj}^Z + K^Z} \right) \right]$ <p><math>HQ</math>: habitat quality; <math>H_j</math>: habitat suitability for habitat type <math>j</math>; <math>D_{xj}</math>: degree of habitat degradation in pixel <math>x</math> that is in habitat type <math>j</math>; <math>K</math>: half-saturation constant; <math>Z</math>: default parameter of the normalized constant model.</p>
CS	InVEST model carbon module	$CS = C_a + C_b + C_s + C_d$ <p><math>CS</math>: carbon storage; <math>C_a</math>, <math>C_b</math>, <math>C_s</math>, and <math>C_d</math> are carbon densities in aboveground biomass, belowground biomass, soil, and dead matter, respectively, for each land use type.</p>

### 2.4. Calculation of Trade-Offs Between Ecosystem Services

Correlation analysis is an effective tool to identify relationships between pairs of ESs, with significant negative correlations representing trade-offs and positive correlations representing synergies [47]. The size of the Pearson correlation coefficient indicates the strength of the trade-off and synergy relationships [47]. Obviously, this method ignores the

difference in the geographical space of the change rate of the ES trade-offs. The root mean squared error (*RMSE*) quantifies the average difference between the standard deviation of a single ES and the average ES's standard deviation [47,48]. The dispersion degree of the standard deviation of distance of average ESs is described, and reflects the difference in the geographical space of the change rate of the ES's trade-offs [49,50]. Therefore, this study uses the *RMSE* to quantify the trade-offs between ESs. To eliminate the influence of ES unit differences, we first standardize the value of each ES.

$$ES_i = \frac{ES_{i,obs} - ES_{i,min}}{ES_{i,max} - ES_{i,min}} \quad (1)$$

where  $ES_i$  is the standardized value;  $ES_{i,obs}$  is the raw value; and  $ES_{i,min}$  and  $ES_{i,max}$  are the minimum and maximum values of the  $i$  ESs, respectively. *RMSE* is calculated as follows:

$$RMSE = \sqrt{\frac{1}{n-1} \sum_{i=1}^n (ES_i - \overline{ES})^2} \quad (2)$$

where  $\overline{ES}$  is the expected value of  $n$  kinds of ESs. In two dimensions, *RMSE* represents the distance from the coordinate point to the diagonal, and the relative position of the coordinate point represents the relative benefit of a certain ecosystem service [49]. Lu et al. [48] and Luo et al. [50] provide detailed instructions and procedures for the calculation of such trade-offs.

### 2.5. Actual Land Use Changes and Scenarios

The local administrative department of the GFGP provided vector data for the implementation area of the GFGP in Lvliang City as of the end of 2018. We set up a scenario where the GFGP was not implemented and quantified the impact of the GFGP on regional ESs by comparing this alternative scenario with the actual scenario.

(1) Actual scenario: we evaluated ESs before (2000) and after (2018) the implementation of the GFGP based on actual land use. By comparing ESs in 2000 and 2018, we can understand actual changes of ESs under the implementation of the GFGP.

(2) Alternative scenarios where the GFGP was not implemented (2018S): this is a simulated scenario. We assume that during the period 2000–2018, the actual GFGP implementation area did not implement the GFGP; that is, the land use types remained, unchanged, at their state in 2000, while the land use types in other regions were consistent with actual changes. By comparing ESs in 2018S and 2018, we were able to quantify the impact of the GFGP on ESs.

Terrain fragmentation due to soil erosion is the main cause of ecological degradation in the Loess Plateau [51]. The design and implementation of the GFGP on the sub-watershed scale to carry out comprehensive control of soil erosion has achieved good results [19,52]. In addition, as a physical geographical unit, the sub-watershed scale can more accurately reflect biophysical characteristics [19]. Therefore, we obtained the average value of each ES at the sub-watershed scale through the Zonal Statistics tool in ArcGIS 10.2. At the sub-watershed scale, the impact of GFGP on ESs was quantified and the trade-offs among ESs and their influencing factors were analyzed.

### 2.6. Geographically Weighted Regression Model

Previous studies have confirmed that there are obvious geographical differences in ESs [53,54]. It is difficult for the classic global regression to reflect the differences in the relationship between ES trade-offs and influencing factors in geographic space, and not fully reflect actual local processes [55]. Geographically weighted regression (GWR) obtains local coefficients by minimizing residuals, taking into account differences in the spatial variation in the relationship between ES trade-offs and influencing factors, which improves the reliability of the model [56].

ESs and their trade-off relationships are affected by factors such as land use [57], climate [58], vegetation [19], geomorphology [59], and urbanization [60]. We selected eight influencing factors to include in our model: the dynamic degree of comprehensive land use change (LUD; Refer to Li et al. [61] method for calculation), annual average temperature (TEM), NDVI, annual average precipitation (PRE), percentage of construction land (CON), elevation (DEM), slope (SLO), and potential evapotranspiration (PET) (Table S4 provides detailed calculation methods or sources). To avoid the influence of multicollinearity, all factors were tested for multicollinearity in SPSS 21, and the factors with VIF greater than five were eliminated (Table S5). These preliminary analyses left us with LUD, NDVI, PRE, DEM, and CON as independent variables and the trade-off relationships between ESs as dependent variables for our GWR model. The lower the  $AIC_c$  value of the model output, the more concise the model and the more reliable the regression estimation. The higher adjusted  $R^2$  indicates a higher explanatory power and a better fit [56]. The mathematical expression of the model is as follows:

$$y_i = \beta_0(u_i, v_i) + \sum_{j=1}^p \beta_j(u_i, v_i)x_{ij} + \varepsilon_i, i \in \{1, 2, \dots, n\} \quad (3)$$

where  $y$  is the dependent variable;  $(u_i, v_i)$  is the spatial location of the  $i$ -th sample;  $\beta_0(u_i, v_i)$  is the intercept;  $p$  is the number of influencing factors;  $x_{ij}$  represents the independent variables;  $\beta_j(u_i, v_i)$  is the estimated coefficient of the  $i$ -th sample for the  $j$ -th driving factors; and  $\varepsilon_i$  is the error term.

### 3. Results

#### 3.1. Land Use Change

Figure 2 shows the land use patterns in 2000, 2018, and 2018S (the scenario if the GFGP were not implemented). Compared with 2000, the area of farmland decreased by 28.90% in 2018, and the area of construction land, forest, grassland, and shrub land increased by 259.31%, 13.7%, 23.98%, and 4.51%, respectively (Table 3). The area of farmland and forest under the 2018S scenario decreased by 5.21% and 10.92%, respectively, and the area of grassland and shrub land increased by 4.20% and 0.87%, respectively (Table 3). Our results show that the GFGP led to a decrease of 23.69% in the area of farmland, and an increase of 24.62%, 19.78%, and 3.64% in the area of forest, grassland, and shrub land, respectively (Table 3), and thus was the main driving force for the significant increase in regional vegetation cover.

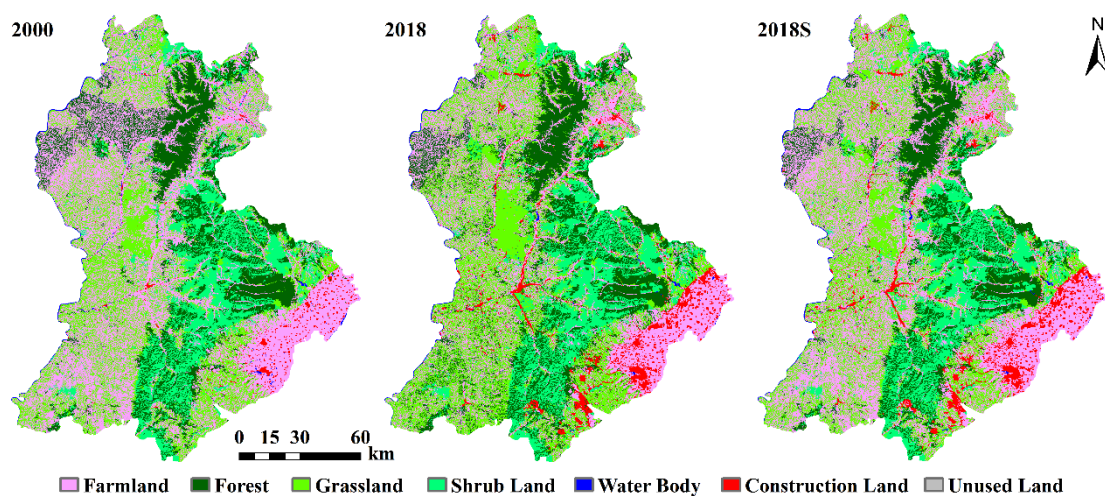


Figure 2. Land use patterns in 2000, 2018, and 2018S. 2018S: the scenario if the GFGP were not implemented.

**Table 3.** Land use changes from 2000 to 2018 and 2018S. 2018S: the scenario if the GFGP were not implemented.

Land Use Types		Farmland	Forest	Grassland	Shrub Land	Water Body	Construction Land	Unused Land
2018	Change area (km <sup>2</sup> )	−2515.04	527.15	1214.05	140.63	−24.39	656.97	0.62
	Change ratio (%)	−28.90%	13.70%	23.98%	4.51%	−17.36%	259.31%	87.06%
2018S	Change area (km <sup>2</sup> )	−453.05	−420.01	212.61	27.23	−24.39	656.97	0.64
	Change ratio (%)	−5.21%	−10.92%	4.20%	0.87%	−17.36%	259.31%	90.36%
Effect of GFGP on land use change (%)		−23.69%	24.62%	19.78%	3.64%	0	0	−3.30%

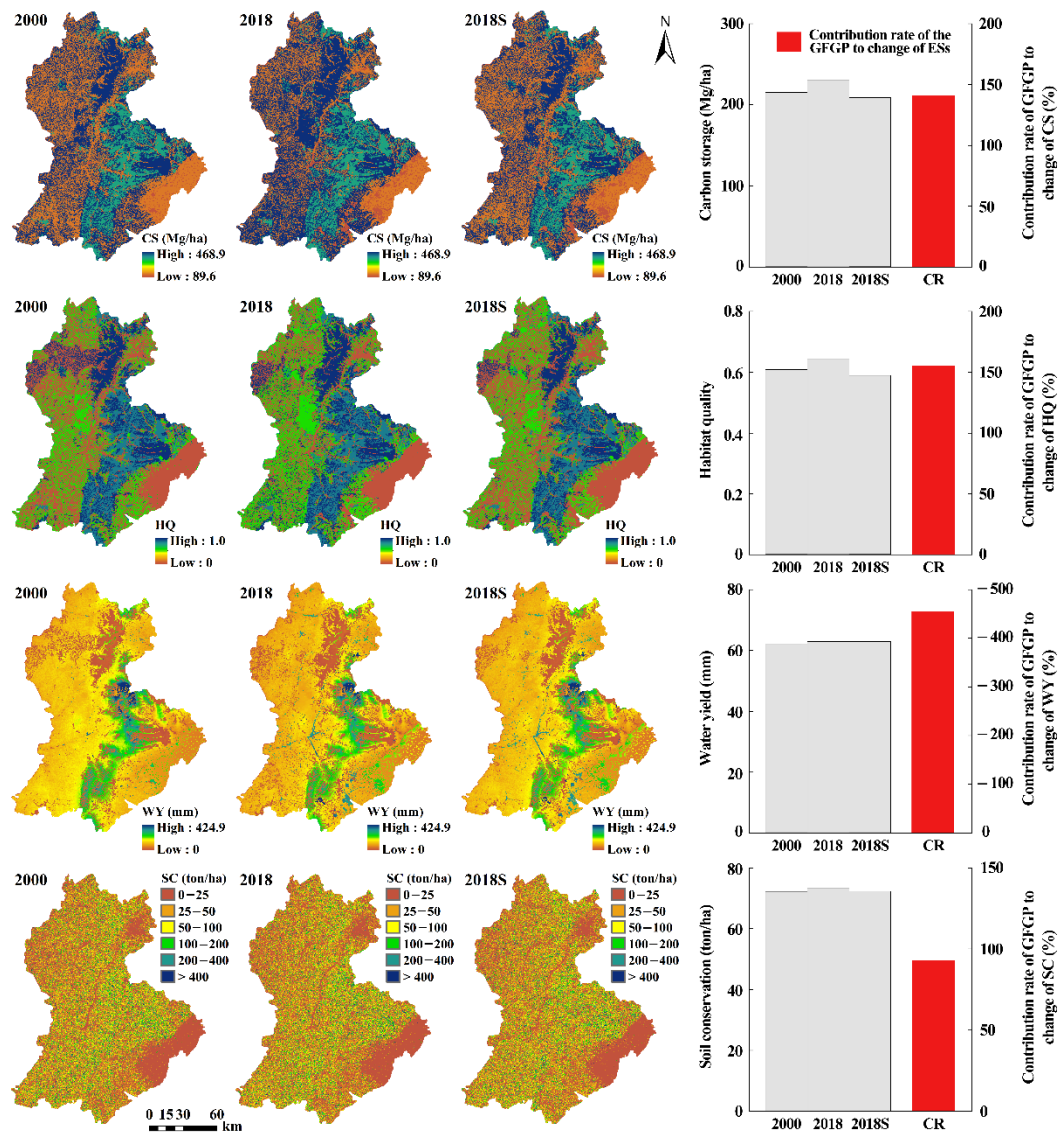
### 3.2. ESs Change

Figure 3 shows the spatial pattern of ESs in 2000, 2018, and 2018S (the scenario if the GFGP were not implemented). The spatial pattern of CS is consistent with land use, and high-value areas are distributed in mountainous regions with higher forest cover (Figure 3). Compared with 2000, the average CS in 2018 and 2018S increased by 15.47 (Mg/ha) and decreased by 6.33 (Mg/ha), respectively. During the study period, the contribution rate of the GFGP to CS changes was 140.92% (Figure 3). The central and eastern areas are dominated by forest and grassland, with high HQ, while in the western loess hilly region and the southeastern plains, HQ is relatively low (Figure 3). Compared with 2000, the average HQ in 2018 and 2018S increased by 0.035 and decreased by 0.019, respectively. During the study period, the contribution rate of the GFGP to HQ changes was 155.59% (Figure 3). WY was high in the center of the study area and low in the outer regions (Figure 3). Compared with 2000, the average WY in 2018 and 2018S increased by 0.79 (mm) and 4.36 (mm), respectively. During the study period, the GFGP had a significant negative impact on WY, with a contribution rate of −454.48% (Figure 3). The central and eastern regions had high SC values, while the southeast and western regions had relatively low SC (Figure 3). Compared with 2000, the average SC in 2018 and 2018S increased by 0.947 (ton/ha) and 0.067 (ton/ha), respectively. During the study period, the contribution rate of the GFGP to SC changes was 92.96% (Figure 3). In general, the implementation of the GFGP from 2000 to 2018 compensated for the negative impacts of external environmental pressures on CS and HQ, and significantly improved CS, HQ, and SC; however, this improvement came at the expense of WY.

### 3.3. Trade-Offs Between ESs

The correlation between changes in ESs from 2000 to 2018 and 2018S (the scenarios if the GFGP were not implemented) was analyzed at the sub-watershed scale. CS, HQ, and SC have a significant synergistic relationship, and there is a significant trade-off between these ESs and WY (Table 4). In addition, the correlation coefficients (including positive and negative correlations) between paired ESs in the actual scenario are larger than those in the alternative scenario if the GFGP were not implemented (Table 4). This indicates that the GFGP has intensified the trade-offs and synergies between ESs.

We visualized the WY-CS, WY-HQ, and WY-SC trade-offs using root mean squared error (RMSE), and our results show that the west and southeast are the high value areas of the trade-offs (Figure 4). Average tradeoff values of WY-CS, WY-HQ, and WY-SC are 0.051, 0.050, and 0.016, respectively, in the actual scenario, and the average tradeoff values of WY-CS, WY-HQ, and WY-SC are 0.028, 0.030, and 0.014, respectively, in the alternative scenario if the GFGP were not implemented (Figure 4). This indicates that the implementation of the GFGP strengthens the trade-offs between WY-CS, WY-HQ, and WY-SC.



**Figure 3.** Spatial pattern of ESs in 2000, 2018, and 2018S. 2018S: the scenario if the GFGP were not implemented. The bar chart on the right represents the average value of ESs in 2000, 2018, and 2018S and the contribution rate of the GFGP to the changes in ESs. Abbreviations: CS: carbon storage; WY: water yield; SC: soil conservation; HQ: habitat quality.

**Table 4.** Pearson’s correlation analysis between changes in ecosystem services.

N = 181	CS2018	HQ2018	SC2018	WY2018	CS2018S	HQ2018S	SC2018S	WY2018S
CS2018	1							
HQ2018	0.920 **	1						
SC2018	0.835 **	0.889 **	1					
WY2018	−0.804 **	−0.898 **	−0.641 **	1				
CS2018S					1			
HQ2018S					0.684 **	1		
SC2018S					0.384 **	0.397 **	1	
WY2018S					−0.645 **	−0.878 **	−0.075	1

CS2018 (CS2018S), HQ2018 (HQ2018S), SC2018 (SC2018S), and WY2018 (WY2018S), respectively, indicate changes in carbon storage, habitat quality, soil conservation, and water yield in 2018 (scenarios with and without the implementation of the GFGP) relative to 2000; N represents the number of sub-watersheds; \*\* indicates significance at the  $p < 0.01$  level.

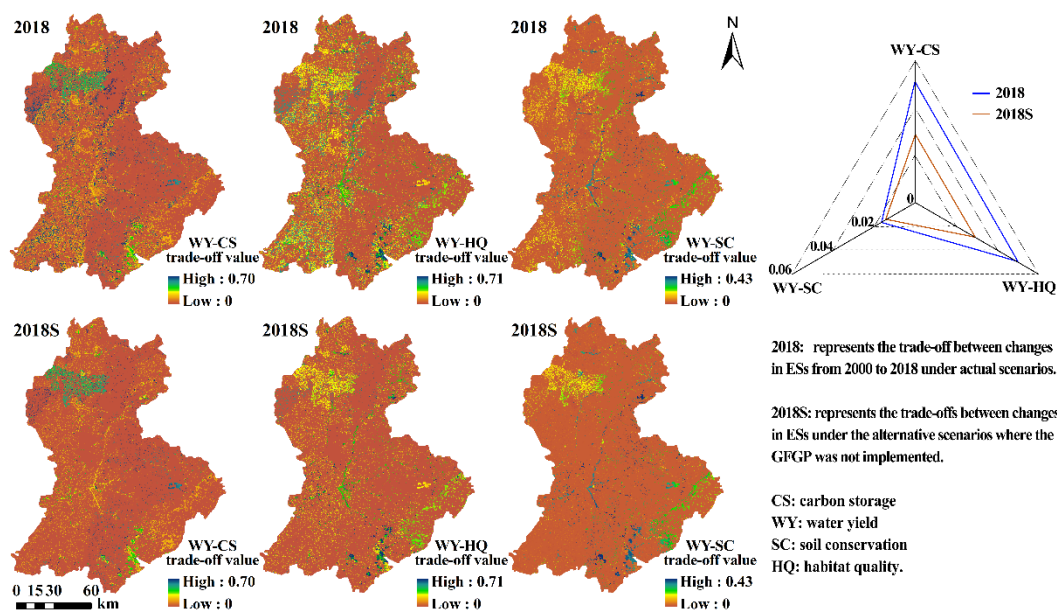


**Figure 4.** The spatial distributions of trade-offs between ESs. The radar graph on the right represents the average values of trade-offs between ESs.

### 3.4. FACTORS Influencing ESs Trade-Offs

We built a GWR model to explore the geospatial relationship between ES trade-offs and the factors that influence them. Compared with OLS, the adjusted  $R^2$  of the GWR model was greater, and the  $AIC_c$  value decreased significantly (Table 5), indicating that the GWR results have higher explanatory power and can more accurately reflect the processes at play.

**Table 5.** Model fit metrics for ordinary least squares (OLS) regression and GWR.

ES Trade-Offs	Fit Metrics	Model	
		OLS	GWR
WY-CS	$R^2$ (adjust)	0.837	0.908
	$AIC_c$	194.958	128.907
WY-HQ	$R^2$ (adjust)	0.901	0.942
	$AIC_c$	104.279	48.576
WY-SC	$R^2$ (adjust)	0.721	0.882
	$AIC_c$	291.957	182.843

Abbreviations: CS: carbon storage; WY: water yield; SC: soil conservation; HQ: habitat quality.

The correlation coefficient of the GWR model reflects the spatial non-stationary response of ES trade-offs to influencing factors (Figure 5). LUD is significantly positively correlated with WY-CS, WY-HQ, and WY-SC trade-offs, and the correlation coefficient is relatively high in the northeast (Figure 5 (a1–a3), Table 6). NDVI is significantly negatively correlated with WY-CS, WY-HQ, and WY-SC trade-offs, and the correlation coefficient is relatively high in the southwest (Figure 5 (b1–b3), Table 6). PRE is positively correlated with WY-CS and WY-HQ trade-offs, but negatively correlated with the WY-SC trade-off, and the correlation coefficient is high in the southeast (Figure 5 (c1–c3), Table 6). DEM is negatively correlated with the WY-HQ trade-off, but positively correlated with WY-CS and WY-SC trade-offs, and the correlation coefficient is larger in the north (Figure 5 (d1–d3), Table 6). CON is negatively correlated with the WY-CS trade-off, but significantly positively correlated with WY-HQ and WY-SC trade-offs, and the correlation coefficient is larger in the south (Figure 5 (e1–e3), Table 6).

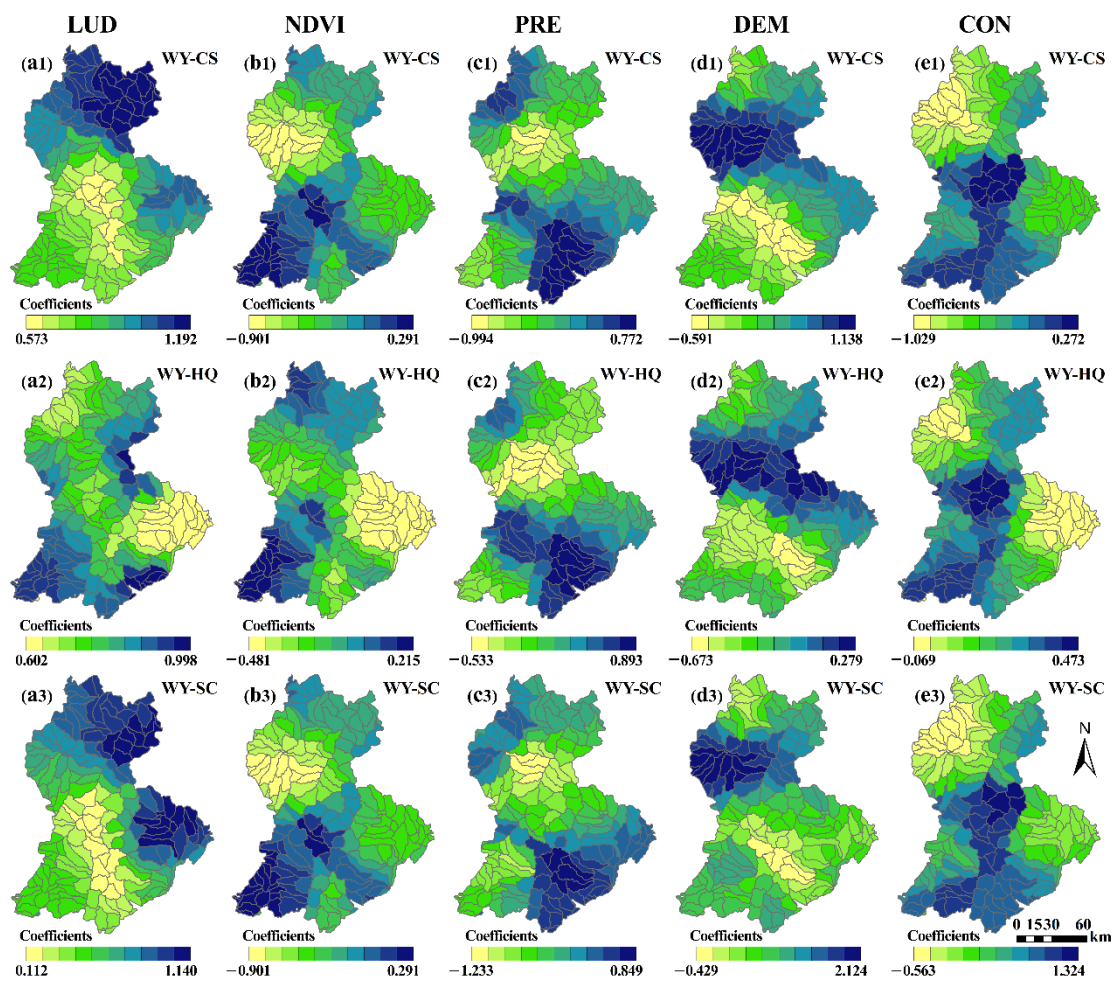


**Figure 5.** GWR coefficients between ES trade-offs and their influencing factors. Abbreviations: CS: carbon storage; WY: water yield; SC: soil conservation; HQ: habitat quality; LUD: dynamic degree of comprehensive land use change; NDVI: Normalized Difference Vegetation Index; PRE: precipitation; DEM: elevation; CON: percentage of construction land.

**Table 6.** Mean statistics of GWR coefficients between ES trade-offs and influencing factors.

ESs Trade-Offs	LUD	NDVI	PRE	DEM	CON
WY-CS	0.888	−0.036	0.044	0.070	−0.143
WY-HQ	0.794	−0.052	0.120	−0.126	0.206
WY-SC	0.595	−0.054	−0.010	0.424	0.619

Abbreviations: CS: carbon storage; WY: water yield; SC: soil conservation; HQ: habitat quality; LUD: dynamic degree of comprehensive land use change; NDVI: Normalized Difference Vegetation Index; PRE: precipitation; DEM: elevation; CON: percentage of construction land.

Local  $R^2$  maps describe spatial differences in model goodness of fit, ranging between 0 and 1. Our results show that the selected five influencing factors are closely related to ES trade-offs, explaining 90.8%, 94.2%, and 88.2% of the WY-CS, WY-HQ, and WY-SC trade-offs, respectively (Figure 6, Table 5). In general, LUD, CON, and NDVI are the most important driving factors of ES trade-offs, and they are significantly positively correlated with LUD and CON while being negatively correlated with NDVI (Figure 6, Table 6). This means that increasing vegetation cover, controlling the intensity of land use change, and optimizing the development of urbanization are effective ways to alleviate the trade-offs between ESs and realize the synergistic promotion of multiple ESs.

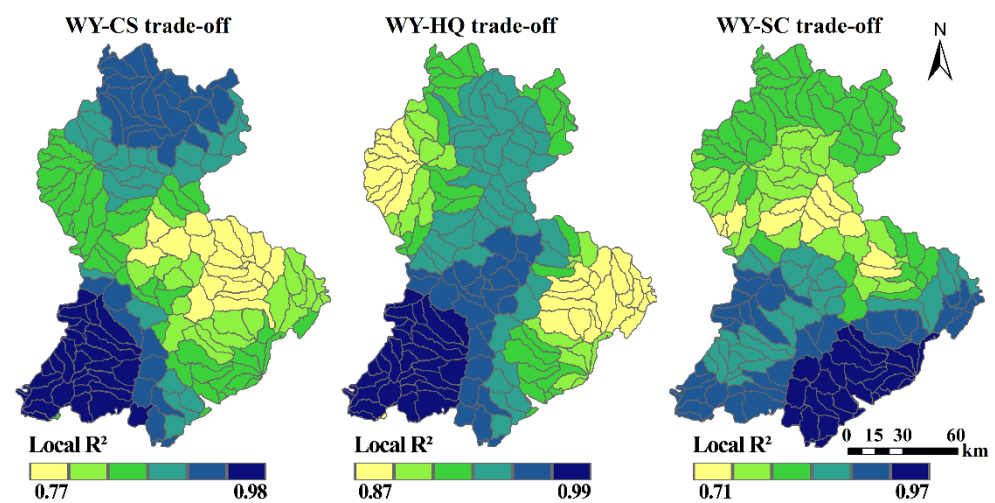


**Figure 6.** Spatial patterns of local  $R^2$  from GWR between ES trade-offs and influencing factors. Abbreviations: CS: carbon storage; WY: water yield; SC: soil conservation; HQ: habitat quality.

## 4. Discussion

### 4.1. Effects of the GFPG on ESs

The GFPG is a successful program for coping with environmental degradation and increasing the supply of ESs [31]. Although the quality of the regional ecological environment has been greatly improved [17,62], realizing the coordinated development of multiple ESs is still a key consideration in optimizing GFPG policies. Our results show that the implementation of the GFPG significantly increased forest, grassland, and shrub land area (Table 3), and vegetation cover increased significantly [24], leading to significant increases in CS, HQ, and SC. This indicates that the GFPG promoted the synergistic relationship among CS, HQ, and SC. However, CS and HQ, under an alternative scenario where the GFPG was not implemented, significantly decreased (Figure 3), indicating that the GFPG effectively compensated for the negative impacts of external environmental pressures on CS and HQ. By comparing the actual scenario in 2018 with the alternative scenario, we found that the GFPG is the most important driving force for the increase in SC, with a contribution rate of 92.96% (Figure 3). In addition, our results show that the GFPG has had a significant negative impact on WY, with a contribution rate of  $-454.48\%$  (Figure 3). This is mainly due to the large-scale planting of non-native vegetation, which leads to a significant increase in water consumption and evapotranspiration [27,63]. Our research confirms that the GFPG produces significant ecological benefits while also exacerbating regional water resource conflicts, which is consistent with previous studies [26,27,51,64]. However, unlike previous studies, we quantified the contribution rate of the GFPG to ES changes and the impact on the trade-offs/synergies between ESs, providing a more direct reference for alleviating regional water resource conflicts and realizing the synergistic promotion of multiple ESs.

### 4.2. Suggestions on the Inclusiveness and Sustainable Development of the GFPG

Identifying the dominant factors influencing the trade-offs between ESs is critical to formulating an inclusive and sustainable plan for the GFPG. There are obvious spatial differences in the relationships between ES trade-offs and their influencing factors [65,66], and classical global regression models did not fully reflect the relationships between the two in geographic space [59]. The local coefficients obtained by the GWR model by minimizing the residuals reflect the spatial non-stationary relationships between them [56], effectively overcoming the problems with classic regression models. We used the GWR model to explore the spatially non-stationary relationship between ES trade-offs and their influencing factors, and our results show that LUD, CON, and NDVI are the most important driving factors for ES trade-offs (Figure 5, Table 6). The WY–CS, WY–HQ, and WY–SC trade-offs

were significantly positively correlated with LUD and CON, but negatively correlated with NDVI (Figure 5 (a1–a3, b1–b3, e1–e3), Table 6).

Land use change and urbanization are the main drivers of declines in CS, HQ, and SC [57,67], and also have negative impacts on the water conservation capacity of ecosystems [68]. However, land use change and urbanization also reduced the evapotranspiration of surface vegetation to a certain degree [69], and their impacts on precipitation at smaller timescales are also limited [70]. Therefore, increases in LUD and CON intensify the trade-offs between WY–CS, WY–HQ, and WY–SC. NDVI is the most direct manifestation of the effectiveness of afforestation [71]. The GFGP is the main driver of the increase in regional NDVI [24], which not only improves CS, HQ, and SC but also improves the water conservation capacity of the ecosystem [72,73]. Therefore, increasing NDVI helps to alleviate the trade-offs between WY–CS, WY–HQ, and WY–SC.

The correlation coefficient of the GWR model reflects the spatial non-stationary response of ES trade-offs to their influencing factors (Figure 5). In the northeast and south of the study area, urbanization developed rapidly and the intensity of human activity was high (Figure 2), so the correlation coefficient between LUD, CON, and ES trade-offs was relatively large (Figure 5 (a1–a3, e1–e3)). In the southwestern region, the terrain is rugged and vegetation is relatively scarce [34], so the correlation coefficient between NDVI and ESs trade-offs is relatively high (Figure 5 (b1–b3)). Therefore, controlling LUD and CON in the northeast and south, and increasing vegetation cover in the southwest, is essential to alleviate the WY–CS, WY–HQ, and WY–SC trade-offs.

In summary, we propose that future engineering projects should take into account the geospatial relationships between ES trade-offs and their influencing factors. By controlling the intensity of land use change, optimizing the development of urbanization, and improving the effectiveness of afforestation, the inclusive and sustainable development of the regional GFGP can be realized.

#### 4.3. Uncertainties and Limitations

Our research provides a direct and flexible method to quantify the impacts of the GFGP on ESs, but it still has certain limitations. First, changing ESs is a complex process driven by factors such as nature, human activities, and climate change [17,74]. It is very difficult to completely quantify the impact of the GFGP on ESs. Our study used the average climate parameters from 2000 to 2018. Although this method is widely adopted [45,46], climate change during the research period will certainly have had an impact on ESs. Second, the input parameters of the model evaluation are taken from previous studies, but due to the limitations of our data sources, quality, and availability, we did not verify the results of the ES evaluations. Third, because of the limited availability of data, we had to ignore some details of the GFGP, such as tree species selection and configuration, vegetation management methods, etc., although these practices certainly could have a strong impact on ESs [71]. These problems may introduce some uncertainty into our model results. Therefore, it is necessary to obtain long-term positioning observation data and conduct more detailed research on the impacts of the GFGP.

## 5. Conclusions

Based on scenario analysis, we quantified the impacts of the GFGP on changes in ESs in Lvliang City, a typical ecologically fragile area, and analyzed the main forces driving ES trade-offs through spatial regression. Our research shows that the GFGP compensated for the negative impacts of external environmental pressures on CS and HQ, and significantly improved CS, HQ, and soil conservation (SC), but this improvement came at the expense of water yield (WY). While the GFGP promotes the synergistic development of CS, HQ, and SC, it also intensifies the trade-off relationships between these services and WY. Land use change and urbanization are significantly positively correlated with the trade-offs between WY–CS, WY–HQ, and WY–SC, while increasing NDVI helped to alleviate these trade-offs. Therefore, controlling the intensity of land use change, optimizing the development of

urbanization, and improving the effectiveness of afforestation are effective ways to realize the inclusive and sustainable development of the GFGP. The general methods used in this study to quantify the impacts of ecological engineering on ESs can provide a reference for future ecological restoration plans and decision-making in China and around the world.

**Supplementary Materials:** The following are available online at <https://www.mdpi.com/article/10.3390/rs13193966/s1>, Table S1: Threats and their maximum distance of influence and weights. Table S2: The sensitivity of habitat types to each threat. Table S3: Table of biophysical coefficients for InVEST. Table S4: Description of variables selected in this study. Table S5: Multicollinearity test among influencing factors.

**Author Contributions:** Conceptualization, Methodology, and Writing—original draft, B.H.; Formal analysis, Z.Z.; Validation and Resources, H.H.; Software and Data curation, Z.L.; Project administration, X.C.; Supervision, F.K.; Visualization, H.W. All authors have read and agreed to the published version of the manuscript.

**Funding:** This research was supported by the National Key Research and Development Program of China (No. 2019YFA0607304).

**Institutional Review Board Statement:** Not applicable.

**Informed Consent Statement:** Not applicable.

**Data Availability Statement:** Publicly available datasets were analyzed in this study. Data sources and access links are detailed in Table 1 and Table S4.

**Acknowledgments:** We sincerely thank the reviewers and editors for their efforts to improve the quality of our paper. We would like to express our gratitude to those who participated in the manuscript revisions.

**Conflicts of Interest:** The authors declare no conflict of interest.

## References

1. Costanza, R.; d'Arge, R.; De Groot, R.; Farber, S.; Grasso, M.; Hannon, B.; Limburg, K.; Naeem, S.; O'Neill, R.V.; Paruelo, J.; et al. The value of the world's ecosystem services and natural capital. *Nature* **1997**, *387*, 253–260. [\[CrossRef\]](#)
2. Carpenter, S.R.; Mooney, H.A.; Agard, J.; Capistrano, D.; Defries, R.S.; Díaz, S.; Dietz, T.; Duraipappah, A.K.; Oteng-Yeboah, A.; Pereira, H.M.; et al. Science for managing ecosystem services: Beyond the millennium ecosystem assessment. *Proc. Natl. Acad. Sci. USA* **2009**, *106*, 1305–1312. [\[CrossRef\]](#) [\[PubMed\]](#)
3. Costanza, R.; De Groot, R.; Sutton, P.; van der Ploeg, S.; Anderson, S.J.; Kubiszewski, I.; Farber, S.; Turner, R.K. Changes in the global value of ecosystem services. *Glob. Environ. Chang.* **2014**, *26*, 152–158. [\[CrossRef\]](#)
4. Xiang, H.; Wang, Z.; Mao, D.; Zhang, J.; Zhao, D.; Zeng, Y.; Wu, F. Surface mining caused multiple ecosystem service losses in China. *J. Environ. Manag.* **2021**, *290*, 112618. [\[CrossRef\]](#) [\[PubMed\]](#)
5. Newbold, T.; Hudson, L.N.; Hill, S.L.L.; Contu, S.; Lysenko, I.; Senior, R.A.; Börger, L.; Bennett, D.J.; Choimes, A.; Collen, B.; et al. Global effects of land use on local terrestrial biodiversity. *Nature* **2015**, *520*, 45–50. [\[CrossRef\]](#)
6. Wunder, S.; Brouwer, R.; Engel, S.; Ezzine-de-Blas, D.; Muradian, R.; Pascual, U.; Pinto, R. From principles to practice in paying for nature's services. *Nat. Sustain.* **2018**, *1*, 145–150. [\[CrossRef\]](#)
7. Zeng, J.; Chen, T.; Yao, X.; Chen, W. Do protected areas improve ecosystem services? A case study of Hoh Xil Nature Reserve in Qinghai-Tibetan Plateau. *Remote Sens.* **2020**, *12*, 471. [\[CrossRef\]](#)
8. Benayas, J.M.R.; Newton, A.C.; Diaz, A.; Bullock, J.M. Enhancement of biodiversity and ecosystem services by ecological restoration: A meta-analysis. *Science* **2009**, *325*, 1121–1124. [\[CrossRef\]](#)
9. Salzman, J.; Bennett, G.; Carroll, N.; Goldstein, A.; Jenkins, M. The global status and trends of Payments for Ecosystem Services. *Nat. Sustain.* **2018**, *1*, 136–144. [\[CrossRef\]](#)
10. Costanza, R.; De Groot, R.; Braat, L.; Kubiszewski, I.; Fioramonti, L.; Sutton, P.; Farber, S.; Grasso, M. Twenty years of ecosystem services: How far have we come and how far do we still need to go? *Ecosyst. Serv.* **2017**, *28*, 1–16. [\[CrossRef\]](#)
11. Gao, J. Editorial for the Special Issue "Ecosystem Services with Remote Sensing". *Remote Sens.* **2020**, *12*, 2191. [\[CrossRef\]](#)
12. Turkelboom, F.; Leone, M.; Jacobs, S.; Kelemen, E.; García-Llorente, M.; Baró, F.; Termansen, M.; Barton, D.N.; Berry, P.; Stange, E.; et al. When we cannot have it all: Ecosystem services trade-offs in the context of spatial planning. *Ecosyst. Serv.* **2018**, *29*, 566–578. [\[CrossRef\]](#)
13. Qian, D.; Du, Y.; Li, Q.; Guo, X.; Cao, G. Alpine grassland management based on ecosystem service relationships on the southern slopes of the Qilian Mountains, China. *J. Environ. Manag.* **2021**, *288*, 112447. [\[CrossRef\]](#) [\[PubMed\]](#)
14. Li, S.; Zhang, Y.; Wang, Z.; Li, L. Mapping human influence intensity in the Tibetan Plateau for conservation of ecological service functions. *Ecosyst. Serv.* **2018**, *30*, 276–286. [\[CrossRef\]](#)

15. Schirpke, U.; Tscholl, S.; Tasser, E. Spatio-temporal changes in ecosystem service values: Effects of land-use changes from past to future (1860–2100). *J. Environ. Manag.* **2020**, *272*, 111068. [[CrossRef](#)]
16. Grafius, D.R.; Corstanje, R.; Warren, P.H.; Evans, K.L.; Hancock, S.; Harris, J.A. The impact of land use/land cover scale on modelling urban ecosystem services. *Landsc. Ecol.* **2016**, *31*, 1509–1522. [[CrossRef](#)]
17. Liu, Y.; Lü, Y.; Fu, B.; Harris, P.; Wu, L. Quantifying the spatio-temporal drivers of planned vegetation restoration on ecosystem services at a regional scale. *Sci. Total. Environ.* **2019**, *650*, 1029–1040. [[CrossRef](#)]
18. Zheng, H.; Li, Y.; Robinson, B.E.; Liu, G.; Ma, D.; Wang, F.; Lu, F.; Ouyang, Z.; Daily, G.C. Using ecosystem service trade-offs to inform water conservation policies and management practices. *Front. Ecol. Environ.* **2016**, *14*, 527–532. [[CrossRef](#)]
19. Feng, Q.; Zhao, W.; Hu, X.; Liu, Y.; Daryanto, S.; Cherubini, F. Trading-off ecosystem services for better ecological restoration: A case study in the Loess Plateau of China. *J. Clean. Prod.* **2020**, *257*, 120469. [[CrossRef](#)]
20. Divinsky, I.; Becker, N.; Kutiel, P. Ecosystem service tradeoff between grazing intensity and other services—A case study in Karei-Deshe experimental cattle range in northern Israel. *Ecosyst. Serv.* **2017**, *24*, 16–27. [[CrossRef](#)]
21. Peng, J.; Hu, X.; Wang, X.; Meersmans, J.; Liu, Y.; Qiu, S. Simulating the impact of Grain-for-Green Programme on ecosystem services trade-offs in Northwestern Yunnan, China. *Ecosyst. Serv.* **2019**, *39*, 100998. [[CrossRef](#)]
22. Cai, W.; Borlace, S.; Lengaigne, M.; Rensch, P.V.; Collins, M.; Vecchi, G.; Timmermann, A.; Santoso, A.; McPhaden, M.J.; Wu, L.; et al. Increasing frequency of extreme El Niño events due to greenhouse warming. *Nat. Clim. Chang.* **2014**, *4*, 111–116. [[CrossRef](#)]
23. Geng, Q.; Ren, Q.; Yan, H.; Li, L.; Zhao, X.; Mu, X.; Wu, P.; Yu, Q. Target areas for harmonizing the Grain for Green Programme in China's Loess Plateau. *Land Degrad. Dev.* **2019**, *31*, 325–333. [[CrossRef](#)]
24. Zheng, K.; Wei, J.; Pei, J.; Cheng, H.; Zhang, X.; Huang, F.; Li, F.; Ye, J. Impacts of climate change and human activities on grassland vegetation variation in the Chinese Loess Plateau. *Sci. Total. Environ.* **2019**, *660*, 236–244. [[CrossRef](#)]
25. Hou, Y.; Lü, Y.; Chen, W.; Fu, B. Temporal variation and spatial scale dependency of ecosystem service interactions: A case study on the central Loess Plateau of China. *Landsc. Ecol.* **2017**, *32*, 1201–1217. [[CrossRef](#)]
26. Wen, X.; Théau, J. Spatiotemporal analysis of water-related ecosystem services under ecological restoration scenarios: A case study in northern Shaanxi, China. *Sci. Total. Environ.* **2020**, *720*, 137477. [[CrossRef](#)] [[PubMed](#)]
27. Feng, X.; Fu, B.; Piao, S.; Wang, S.; Ciais, P.; Zeng, Z.; Lü, Y.; Zeng, Y.; Li, Y.; Jiang, X.; et al. Revegetation in China's Loess Plateau is approaching sustainable water resource limits. *Nat. Clim. Chang.* **2016**, *6*, 1019–1022. [[CrossRef](#)]
28. Chen, Y.; Wang, K.; Lin, Y.; Shi, W.; Song, Y.; He, X. Balancing green and grain trade. *Nat. Geosci.* **2015**, *8*, 739–741. [[CrossRef](#)]
29. Yang, S.; Bai, Y.; Alatalo, J.M.; Wang, H.; Jiang, B.; Liu, G.; Chen, G. Spatio-temporal changes in water-related ecosystem services provision and trade-offs with food production. *J. Clean. Prod.* **2021**, *286*, 125316. [[CrossRef](#)]
30. Mandle, L.; Shields-Estrada, A.; Chaplin-Kramer, R.; Mitchell, M.G.E.; Bremer, L.L.; Gourevitch, J.D.; Hawthorne, P.; Johnson, J.A.; Robinson, B.E.; Smith, J.R.; et al. Increasing decision relevance of ecosystem service science. *Nat. Sustain.* **2021**, *4*, 161–169. [[CrossRef](#)]
31. Ouyang, Z.; Zheng, H.; Xiao, Y.; Polasky, S.; Liu, J.; Xu, W.; Wang, Q.; Zhang, L.; Xiao, Y.; Rao, E.; et al. Improvements in ecosystem services from investments in natural capital. *Science* **2016**, *352*, 1455–1459. [[CrossRef](#)]
32. Yang, S.; Zhao, W.; Liu, Y.; Wang, S.; Wang, J.; Zhai, R. Influence of land use change on the ecosystem service trade-offs in the ecological restoration area: Dynamics and scenarios in the Yanhe watershed, China. *Sci. Total. Environ.* **2018**, *644*, 556–566. [[CrossRef](#)]
33. Peng, J.; Tian, L.; Zhang, Z.; Zhao, Y.; Green, S.M.; Quine, T.A.; Liu, H.; Meersmans, J. Distinguishing the impacts of land use and climate change on ecosystem services in a karst landscape in China. *Ecosyst. Serv.* **2020**, *46*, 101199. [[CrossRef](#)]
34. Sun, C.; Li, X.; Zhang, W.; Chen, W.; Wang, J. Evaluation of ecological security in poverty-stricken region of Lüliang Mountain based on the remote sensing image. *China Environ. Sci.* **2019**, *39*, 5352–5360.
35. Li, J.; Wang, Y. Spatial coupling characteristics of eco-environment quality and economic poverty in Lüliang area. *Chin. J. Appl. Ecol.* **2014**, *25*, 1715–1724.
36. Sharp, R.; Tallis, H.T.; Ricketts, T.; Guerry, A.D.; Wood, S.A.; Chaplin-Kramer, R.; Nelson, E.; Ennaanay, D.; Wolny, S.; Olwero, N.; et al. InVEST 3.8.0 User's Guide. The Natural Capital Project: Stanford University, University of Minnesota, The Nature Conservancy, and World Wildlife Fund. 2020. Available online: <http://releases.naturalcapitalproject.org/invest-userguide/latest/#supporting-tools> (accessed on 26 November 2020).
37. Zhang, L.; Fu, B.; Lü, Y.; Zeng, Y. Balancing multiple ecosystem services in conservation priority setting. *Landsc. Ecol.* **2015**, *30*, 535–546. [[CrossRef](#)]
38. Liu, L.; Zhang, H.; Gao, Y.; Zhu, W.; Liu, X.; Xu, Q. Hotspot identification and interaction analyses of the provisioning of multiple ecosystem services: Case study of Shaanxi Province, China. *Ecol. Indic.* **2019**, *107*, 105566. [[CrossRef](#)]
39. Sun, X.; Lu, Z.; Li, F.; Crittenden, J.C. Analyzing spatio-temporal changes and trade-offs to support the supply of multiple ecosystem services in Beijing, China. *Ecol. Indic.* **2018**, *94*, 117–129. [[CrossRef](#)]
40. Liu, C.; Wang, C. Spatio-temporal evolution characteristics of habitat quality in the Loess Hilly Region based on land use change: A case study in Yuzhong county. *Acta Ecol. Sin.* **2018**, *38*, 7300–7311.
41. Zhou, L.; Tang, J.; Liu, X.; Dang, X.; Mu, H. Effects of urban expansion on habitat quality in densely populated areas on the Loess Plateau: A case study of Lanzhou, Xi'an-Xianyang and Taiyuan, China. *Chin. J. Appl. Ecol.* **2021**, *32*, 261–270.
42. Liang, Y.; Hashimoto, S.; Liu, L. Integrated assessment of land-use/land-cover dynamics on carbon storage services in the Loess Plateau of China from 1995 to 2050. *Ecol. Indic.* **2021**, *120*, 106939. [[CrossRef](#)]

43. Zhang, Y.; Shi, X.; Tang, Q. Carbon storage assessment in the upper reaches of the Fenhe River under different land use scenarios. *Acta Ecol. Sin.* **2021**, *41*, 360–373.
44. Tang, X.; Zhao, X.; Bai, Y.; Tang, Z.; Wang, W.; Zhao, Y.; Wan, H.; Xie, Z.; Shi, X.; Wu, B.; et al. Carbon pools in China's terrestrial ecosystems: New estimates based on an intensive field survey. *Proc. Natl. Acad. Sci. USA* **2018**, *115*, 4021–4026. [[CrossRef](#)] [[PubMed](#)]
45. Zheng, H.; Wang, L.; Peng, W.; Zhang, C.; Li, C.; Robinson, B.E.; Wu, X.; Kong, L.; Li, R.; Xiao, Y.; et al. Realizing the values of natural capital for inclusive, sustainable development: Informing China's new ecological development strategy. *Proc. Natl. Acad. Sci. USA* **2019**, *116*, 8623–8628. [[CrossRef](#)]
46. Fu, Q.; Li, B.; Hou, Y.; Bi, X.; Zhang, X. Effects of land use and climate change on ecosystem services in Central Asia's arid regions: A case study in Altay Prefecture, China. *Sci. Total. Environ.* **2017**, *607*, 633–646. [[CrossRef](#)] [[PubMed](#)]
47. Bradford, J.B.; D'Amato, A.W. Recognizing trade-offs in multi-objective land management. *Front. Ecol. Environ.* **2012**, *10*, 210–216. [[CrossRef](#)]
48. Lu, N.; Fu, B.; Jin, T.; Chang, R. Trade-off analyses of multiple ecosystem services by plantations along a precipitation gradient across Loess Plateau landscapes. *Landsc. Ecol.* **2014**, *29*, 1697–1708. [[CrossRef](#)]
49. Xu, J.; Chen, J.; Liu, Y. Partitioned responses of ecosystem services and their tradeoffs to human activities in the Belt and Road region. *J. Clean. Prod.* **2020**, *276*, 123205.
50. Luo, Y.; Lü, Y.; Fu, B.; Zhang, Q.; Li, T.; Hu, W.; Comber, A. Half century change of interactions among ecosystem services driven by ecological restoration: Quantification and policy implications at a watershed scale in the Chinese Loess Plateau. *Sci. Total. Environ.* **2019**, *651*, 2546–2557. [[CrossRef](#)]
51. Fu, B.; Wang, S.; Liu, Y.; Liu, J.; Liang, W.; Miao, C. Hydrogeomorphic ecosystem responses to natural and anthropogenic changes in the Loess Plateau of China. *Annu. Rev. Earth Planet. Sci.* **2017**, *45*, 223–243. [[CrossRef](#)]
52. Jiang, C.; Zhang, H.; Zhang, Z. Spatially explicit assessment of ecosystem services in China's Loess Plateau: Patterns, interactions, drivers, and implications. *Glob. Planet. Chang.* **2018**, *161*, 41–52. [[CrossRef](#)]
53. Wang, L.; Ma, S.; Jiang, J.; Zhao, Y.; Zhang, J. Spatiotemporal Variation in Ecosystem Services and Their Drivers among Different Landscape Heterogeneity Units and Terrain Gradients in the Southern Hill and Mountain Belt, China. *Remote Sens.* **2021**, *13*, 1375. [[CrossRef](#)]
54. Ahmed, M.A.; Abd-Elrahman, A.; Escobedo, F.J.; Cropper, W.P.; Martin, T.A.; Timilsina, N. Spatially-explicit modeling of multi-scale drivers of aboveground forest biomass and water yield in watersheds of the Southeastern United States. *J. Environ. Manag.* **2017**, *199*, 158–171. [[CrossRef](#)] [[PubMed](#)]
55. Zhang, Z.; Liu, Y.; Wang, Y.; Liu, Y.; Zhang, Y.; Zhang, Y. What factors affect the synergy and tradeoff between ecosystem services, and how, from a geospatial perspective? *J. Clean. Prod.* **2020**, *257*, 120454. [[CrossRef](#)]
56. Fotheringham, A.S.; Yang, W.; Kang, W. Multiscale geographically weighted regression (MGWR). *Ann. Am. Assoc. Geogr.* **2017**, *107*, 1247–1265. [[CrossRef](#)]
57. Clerici, N.; Cote-Navarro, F.; Escobedo, F.J.; Rubiano, K.; Villegas, J.C. Spatio-temporal and cumulative effects of land use-land cover and climate change on two ecosystem services in the Colombian Andes. *Sci. Total. Environ.* **2019**, *685*, 1181–1192. [[CrossRef](#)] [[PubMed](#)]
58. Sannigrahi, S.; Zhang, Q.; Pilla, F.; Joshi, P.K.; Basu, B.; Keesstra, S.; Roy, P.S.; Wang, Y.; Sutton, P.C.; Chakraborti, S.; et al. Responses of ecosystem services to natural and anthropogenic forcings: A spatial regression based assessment in the world's largest mangrove ecosystem. *Sci. Total. Environ.* **2020**, *715*, 137004. [[CrossRef](#)]
59. Gao, J.; Zuo, L.; Liu, W. Environmental determinants impacting the spatial heterogeneity of karst ecosystem services in Southwest China. *Land Degrad. Dev.* **2020**, *32*, 1718–1731. [[CrossRef](#)]
60. Li, S.; He, Y.; Xu, H.; Zhu, C.; Dong, B.; Lin, Y.; Si, B.; Deng, J.; Wang, K. Impacts of Urban Expansion Forms on Ecosystem Services in Urban Agglomerations: A Case Study of Shanghai-Hangzhou Bay Urban Agglomeration. *Remote Sens.* **2021**, *13*, 1908. [[CrossRef](#)]
61. Li, B.; Wang, W. Trade-offs and synergies in ecosystem services for the Yinchuan Basin in China. *Ecol. Indic.* **2018**, *84*, 837–846. [[CrossRef](#)]
62. Guo, S.; Han, X.; Li, H.; Wang, T.; Tong, X.; Ren, G.; Feng, Y.; Yang, G. Evaluation of soil quality along two revegetation chronosequences on the Loess Hilly Region of China. *Sci. Total. Environ.* **2018**, *633*, 808–815. [[CrossRef](#)] [[PubMed](#)]
63. Yang, L.; Che, L.; Wei, W.; Yu, Y.; Zhang, H. Comparison of deep soil moisture in two re-vegetation watersheds in semi-arid regions. *J. Hydrol.* **2014**, *513*, 314–321. [[CrossRef](#)]
64. Jia, X.; Fu, B.; Feng, X.; Hou, G.; Liu, Y.; Wang, X. The tradeoff and synergy between ecosystem services in the Grain-for-Green areas in Northern Shaanxi, China. *Ecol. Indic.* **2014**, *43*, 103–113. [[CrossRef](#)]
65. Garcia, A.M.; Santé, I.; Loureiro, X.; Miranda, D. Green infrastructure spatial planning considering ecosystem services assessment and trade-off analysis. Application at landscape scale in Galicia region (NW Spain). *Ecosyst. Serv.* **2020**, *43*, 101115. [[CrossRef](#)]
66. Liang, J.; Li, S.; Li, X.; Li, X.; Liu, Q.; Meng, Q.; Lin, A.; Li, J. Trade-off analyses and optimization of water-related ecosystem services (WRESs) based on land use change in a typical agricultural watershed, southern China. *J. Clean. Prod.* **2021**, *279*, 123851. [[CrossRef](#)]
67. Wang, X.; Yan, F.; Su, F. Impacts of Urbanization on the Ecosystem Services in the Guangdong-Hong Kong-Macao Greater Bay Area, China. *Remote Sens.* **2020**, *12*, 3269. [[CrossRef](#)]

68. Zhang, Y.; Liu, Y.; Zhang, Y.; Liu, Y.; Zhang, G.; Chen, Y. On the spatial relationship between ecosystem services and urbanization: A case study in Wuhan, China. *Sci. Total. Environ.* **2018**, *637–638*, 780–790. [[CrossRef](#)]
69. Gao, J.; Li, F.; Gao, H.; Zhou, C.; Zhang, X. The impact of land-use change on water-related ecosystem services: A study of the Guishui River Basin, Beijing, China. *J. Clean. Prod.* **2017**, *163*, S148–S155. [[CrossRef](#)]
70. Lang, Y.; Song, W.; Zhang, Y. Responses of the water-yield ecosystem service to climate and land use change in Sancha River Basin, China. *Phys. Chem. Earth* **2017**, *101*, 102–111. [[CrossRef](#)]
71. Wu, X.; Wang, S.; Fu, B.; Liu, J. Spatial variation and influencing factors of the effectiveness of afforestation in China's Loess Plateau. *Sci. Total. Environ.* **2021**, *771*, 144904. [[CrossRef](#)]
72. Wen, X.; Deng, X.; Zhang, F. Scale effects of vegetation restoration on soil and water conservation in a semi-arid region in China: Resources conservation and sustainable management. *Resour. Conserv. Recycl.* **2019**, *151*, 104474. [[CrossRef](#)]
73. Zhou, G.; Wei, X.; Chen, X.; Zhou, P.; Liu, X.; Xiao, Y.; Sun, G.; Scott, D.F.; Zhou, S.; Han, L.; et al. Global pattern for the effect of climate and land cover on water yield. *Nat. Commun.* **2015**, *6*, 5918. [[CrossRef](#)] [[PubMed](#)]
74. He, Y.; Kuang, Y.; Zhao, Y.; Ruan, Z. Spatial Correlation between Ecosystem Services and Human Disturbances: A Case Study of the Guangdong–Hong Kong–Macao Greater Bay Area, China. *Remote Sens.* **2021**, *13*, 1174. [[CrossRef](#)]